ELSEVIER

Inorganica Chimica Acta 338 (2002) 201–209

Inorganica Chimica Acta

www.elsevier.com/locate/ica

Cationic nickel(II) complexes with azine diphosphines—structural and electrochemical study

Fernanda M.T. Almeida [a], M. Fernanda N.N. Carvalho [a], Adelino M. Galvão [a], Jan Čermák [b,*], Vratislav Blechta [b], Armando J.L. Pombeiro [a], Bernard L. Shaw [c]

[a] *Centro de Química Estrutural, Complexo I, Instituto Superior Técnico, Av. Rovisco Pais, 1049-001 Lisbon, Portugal*
[b] *Institute of Chemical Process Fundamentals, Academy of Sciences of the Czech Republic, Rozvojova 135, CZ-16502 Prague 6, Suchdol, Czech Republic*
[c] *University of Leeds, Leeds LS2 9JT, UK*

Received 18 February 2002; accepted 8 April 2002

Abstract

Nickel(II) complexes of azine diphosphine ligands, $PR_2CH_2C(Bu^t)NNC(Bu^t)CH_2PR_2$ ($R = Ph$, Bu^t, Pr^i, C_6H_{11}), were prepared for the first time by reactions of anhydrous NiX_2 ($X = Cl$, Br, I) with ligands. Complexes are cationic, the counterion being either simple halide anion or, in two cases, $1/2[NiCl_4]^{2-}$. The azine diphosphines are coordinated terdentately in (E,Z) configuration forming thereby a bicyclic ligand frame (five and six-membered ring) with diphosphine bite angles 160–165°. A balance of stereoelectronic factors governing square planar versus tetrahedral coordination of the ligands is suggested. Structures of four of the complexes with bulky ligands ($R = Bu^t$, $X^- = Cl^-$, Br^-, I^-; $R = C_6H_{11}$, $X^- = 1/2[NiCl]^{2-}$) were determined by X-ray diffraction and qualitative Hückel MO calculations on model undistorted square planar $[trans\text{-}NiX(NH_2)(PH_3)_2]^+$ were carried out to elucidate the contributions of steric and electronic factors. Two reduction and two oxidation processes depending on the substituent R and the halide were identified from cyclic voltammetry data on the complexes.

Keywords: Diphosphines; Bite angle; Nickel complexes; PNP ligands; Cyclic voltammetry

1. Introduction

Transition metal complexes with rigid terdentate X–Y–Z ligands (sometimes called ‘pincer ligand’) are of considerable interest in organometallic chemistry and catalysis by transition metals and were extensively studied by several groups in recent years. Various combinations of hard or soft atoms X, Y, Z are possible.

Van Koten and coworkers introduced a combination of two nitrogen atoms and one carbon atom to form an N–C–N ligand frame supplying the transition metal center with electron density while at the same time keeping it in a strictly T-shape ligand environment [1]. The ligand frame was used to prepare active nickel catalysts for the Kharasch addition of halomethanes to alkenes; dendritic versions of the catalysts were also developed, manganese(II) complex was used as a catalyst in cross-coupling of Grignard reagents with alkyl bromides [2].

A similar P–C–P ligand backbone was studied by Milstein et al. in a search for stoichiometric and possibly catalytic activation of strong bonds, not amenable to activation by usual means. In this way, solvent-controlled selectivity towards C–H or C–C activation [3], as well as $C–CF_3$ bond activation [4] and C–Si [5] bond activation, were achieved.

The pioneering work of the two above mentioned groups has been extended recently to other donor atom combinations like, e.g. P–C–N [6], O–C–O [7], S–C–S [8] and P–O–P [9]. All the so far mentioned ligand frames share a common feature, which is the formation of two annulated, equal-size metallarings (usually five-membered).

Shaw and coworkers [10–12] developed a terdentate P–N–P ligand, bis(diphenylphosphino)pinacolone azine, which coordinates to metals with formation of

---

* Corresponding author. Fax: +420-2-2092 0661
E-mail address: cermak@icpf.cas.cz (J. Čermák).

0020-1693/02/$ - see front matter © 2002 Elsevier Science B.V. All rights reserved.
PII: S0020-1693(02)00982-9

two unequal-size condensed metallarings. In such complexes, the two phosphine arms of different lengths are expected to have different coordination properties. This is a good basis for increased stoichiometric and possibly catalytic reactivity of the complexes. In addition, the ability of the ligand to promote migration of a proton from ligand backbone to metal [13] or another ligand [14] results in the even more rigid ene-hydrazone coordination mode.

Recently, we synthesized four new bis(dialkyl- or diarylphosphino)pinacolone azines and their chloro(η^3-methallyl)palladium complexes. In this case, the azine diphosphine ligands bridged two palladium units, in agreement with their recognized high coordination versatility. The electronic and steric properties of the complexes were examined by NMR [15].

We now extend the study of the coordination ability of bis(dialkyl- or diarylphosphino)pinacolone azines to nickel. The syntheses and characterization of new cationic chloro–, bromo–, and iodo–Ni(II) complexes of the type $[NiX(P–N–P)]^+X^-$, with several azine diphosphines ($P–N–P = R_2PCH_2C(Bu^t)=N–N=C(Bu^t)–CH_2PR_2$; R = *tert*-butyl, *iso*-propyl, cyclohexyl, phenyl) are reported. In order to fully characterize the compounds the crystal structures of four of them (R = Bu^t, X = Cl, Br or I and R = cyclohexyl, X = Cl) were determined by X-ray diffraction.

The effect of the R groups on the redox properties of the complexes was studied by cyclic voltammetry.

2. Experimental

2.1. Materials and methods

All the manipulations were carried out under argon or dinitrogen atmosphere using standard Schlenk glassware techniques. The solvents were dried by standard methods before use. Anhydrous nickel(II) halides [16], except nickel(II) iodide (Aldrich) and bis(dialkylphosphino)pinacolone azines [15], were prepared by published methods.

The NMR spectra were recorded on a Varian UNITY 200 spectrometer at 200.1, 50.3, and 81.0 MHz for ^1H, ^{13}C and ^{31}P, respectively, or on a Varian UNITY 500 spectrometer at 499.9 and 125.7 MHz for ^1H and ^{13}C, respectively. The spectra were referenced to internal hexamethyldisilane (^1H, $\delta = 0.04$ and ^{13}C, $\delta = -2.49$) or external H_3PO_4 (^{31}P, $\delta = 0.0$).

Mass spectra were measured with Varian CH5 (EI mode, 70 eV) and LCQ Finnigan (ESI) instruments.

The electrochemical studies were performed at an EG&G PAR 173 potentiostat/galvanostat and an EG&G PARC 175 universal programmer, using a 0.2 M $[NBu_4][BF_4]$–THF or CH_2Cl_2 solution and a Pt-wire as the working electrode. The potential values were measured by using the $[Fe(\eta^5\text{-}C_5H_5)_2]^{0/+}$ redox couple ($E = 0.54$ V vs. SCE) as internal standard.

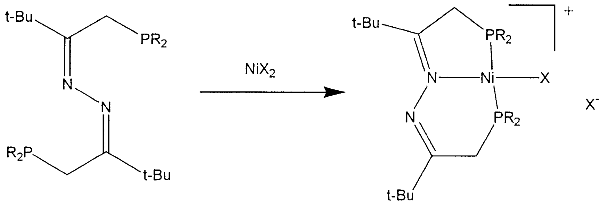

R = Ph, X = Cl, **1a**
R = Ph, X = Br, **1b**
R = Ph, X = I, **1c**
R = Bu^t, X = Cl, **2a**
R = Bu^t, X = Br, **2b**
R = Bu^t, X = I, **2c**

R = Pr^i, X = Cl, **3a**
R = Pr^i, X = Br, **3b**
R = Pr^i, X = I, **3c**
R = c-C_6H_{11}, X = Cl, X^-=1/2 $[NiCl_4]^{2-}$, **4a**
R = c-C_6H_{11}, X = Br, **4b**
R = c-C_6H_{11}, X = I, **4c**

Scheme 1. Synthesis of cationic nickel(II) complexes.

Table 1
Reaction conditions (Scheme 1)

R	X		Reaction time (h)	Yield (%)
Ph	Cl	**1a**	3	49
	Br	**1b**	3 [a]	72
	I	**1c**	0.5	45
Bu^t	Cl	**2a**	3	94
	Br	**2b**	1.5	97
	I	**2c**	2.5	72
Pr^i	Cl	**3a**	24 [a]	45
	Br	**3b**	24 [a]	77
	I	**3c**	24 [a]	37
C_6H_{11}	Cl	**4a**	2	64
	Br	**4b**	2	95
	I	**4c**	2	41

[a] Ambient temperature.

The magnetic susceptibilities were measured at room temperature (r.t.) using a Johnson Matthey magnetic susceptibility balance.

2.2. Syntheses of the azine diphosphines nickel complexes

As a general procedure, dry acetone (20–30 ml g^{-1} of azine diphosphine) was added to equimolar amounts of azine diphosphine and anhydrous nickel(II) halide and the mixture stirred at r.t. or under reflux for a variable period of time. After cooling to ambient temperature (if necessary) a small amount of precipitate was filtered off, the solution was evaporated to approximately half of the initial volume and an equivalent volume of dry diethyl ether was added. After several days, a precipitate appeared that was filtered off and dried under vacuum. In order to obtain analytically pure samples, the products were recrystallized from chloroform–diethyl ether.

The reaction time, temperature and isolated yields of the products (Scheme 1) are displayed in Table 1.

Suitable crystals for X-ray analysis were obtained directly from the reaction solution for **2c** and **4a**, while for **2a** and **2b**, the crystals were obtained upon recrystallization from chloroform–diethyl ether using the technique of solvent diffusion from gas phase.

2.2.1. Characterization of products

*2.2.1.1. $[\mathrm{NiCl\{PPh_2CH_2C(Bu^t)NNC(Bu^t)CH_2PPh_2\}}]_2[\mathrm{NiCl_4}]$ (**1a**).* *Anal*. Calc. for **1a**·1.5CHCl$_3$ ($\mathrm{C_{72}H_{84}Cl_6N_4P_4Ni_3\cdot 1.5CHCl_3}$): C, 52.0; H, 5.1; N, 3.3. Found: C, 52.3; H, 5.4; N, 3.2%.

Mass spectrum (FAB), *m*/*z*: 657 (M^+–Cl), 163 (NiCl$_3$).

*2.2.1.2. $[\mathrm{NiBr\{PPh_2CH_2C(Bu^t)NNC(Bu^t)CH_2PPh_2\}}]\mathrm{Br}$ (**1b**).* *Anal*. Calc. for **1b**·CHCl$_3$ ($\mathrm{C_{36}H_{42}Br_2N_2P_2Ni\cdot CHCl_3}$): C, 49.2; H, 4.8; N, 3.1. Found: C, 49.3; H, 5.1; N, 3.0%.

Mass spectrum (FAB), *m*/*z*: 703 (M^+–Br).

*2.2.1.3. $[\mathrm{NiI\{PPh_2CH_2C(Bu^t)NNC(Bu^t)CH_2PPh_2\}}]\mathrm{I}$ (**1c**).* *Anal*. Calc. for **1c**·0.75CHCl$_3$ ($\mathrm{C_{36}H_{42}I_2N_2P_2Ni\cdot 0.75CHCl_3}$): C, 45.6; H, 4.4; N, 2.9. Found: C, 45.8; H, 4.6; N, 2.5%.

Mass spectrum (FAB), *m*/*z*: 749 (M^+–I).

$^{31}\mathrm{P}\{^1\mathrm{H}\}$ NMR (CDCl$_3$): 46.3, 51.0 (AB system, $^2J_{\mathrm{PP}} = 344$ Hz); ^{1}H NMR (CDCl$_3$): 0.65 (s, 9H), 1.02 (s, 9H), 3.43 (b, $^2J_{\mathrm{PH}} =$ ca. 8 Hz, 2H), 4.41 (b, 4H), 7.3–8.2 (bm, 20H); $^{13}\mathrm{C}\{^1\mathrm{H}\}$ NMR (CDCl$_3$): 26.10 (d, $^1J_{\mathrm{PC}} = 12.0$ Hz, CH$_2$), 26.72 (s, CH$_3$), 28.06 (s, CH$_3$), 40.18 (s, $C(\mathrm{CH_3})_3$), 40.43 (s, $C(\mathrm{CH_3})_3$), 46.18 (d, $^1J_{\mathrm{PC}} = 25.2$ Hz, CH$_2$), 128.10 (d, $J = 8.7$ Hz, –CH=), 128.62 (d, $J = 6.9$ Hz, –CH=), 128.65 (d, $J =$ ca. 45 Hz, >CH=), 129.63 (d, $J =$ ca. 45 Hz, >CH=), 131.53 (d, $J = 19.2$ Hz, –CH=), 134.32 (d, $J =$ ca. 6 Hz, –CH=), 135.66 (s, –CH=), 171.77 (s, C=N), 186.31 (s, C=N).

*2.2.1.4. $[\mathrm{NiCl\{PBu^t_2CH_2C(Bu^t)NNC(Bu^t)CH_2PBu^t_2\}}]\mathrm{Cl}$ (**2a**).* $^{31}\mathrm{P}\{^1\mathrm{H}\}$ NMR (CDCl$_3$): 64.4, 70.5 (AB system $^2J_{\mathrm{PP}} = 325$ Hz); ^{1}H NMR (CDCl$_3$): 1.38 (s, 18H), 1.66 (b, 36H), 2.32 (b, 2H), 4.00 (b, 2H); $^{13}\mathrm{C}\{^1\mathrm{H}\}$ NMR (CDCl$_3$): 14.75 (s, CH$_2$), 28.05 (s, $\mathrm{C}(C\mathrm{H_3})_3$), 28.81 (s, $\mathrm{C}(C\mathrm{H_3})_3$), 29.35 (s, $\mathrm{PC}(C\mathrm{H_3})_3$), 29.90 (d, $^2J_{\mathrm{PC}} = 1.5$ Hz, $\mathrm{PC}(C\mathrm{H_3})_3$), 35.82 (d, $^1J_{\mathrm{PC}} = 16.1$ Hz, CH$_2$), 36.85 (dd, $^1J_{\mathrm{PC}} = 10.6$ Hz, $^3J_{\mathrm{PC}} = 3.5$ Hz, $\mathrm{P}C(\mathrm{CH_3})_3$), 37.1 (dd, $^1J_{\mathrm{PC}} = 9.3$ Hz, $^3J_{\mathrm{PC}} = 2.9$ Hz, $\mathrm{P}C(\mathrm{CH_3})_3$), 41.51 (d, $^3J_{\mathrm{PC}} = 3.9$ Hz, $C(\mathrm{CH_3})_3$), 41.64 (d, $^3J_{\mathrm{PC}} = 2.0$ Hz, $C(\mathrm{CH_3})_3$), 177.48 (s, C=N), 191.22 (s, C=N).

*2.2.1.5. $[\mathrm{NiBr\{PBu^t_2CH_2C(Bu^t)NNC(Bu^t)CH_2PBu^t_2\}}]\mathrm{Br}$ (**2b**).* $^{31}\mathrm{P}\{^1\mathrm{H}\}$ NMR (CDCl$_3$): 68.7, 75.0 (AB system $^2J_{\mathrm{PP}} = 322$ Hz); ^{1}H NMR (CDCl$_3$): 1.43 (s, 9H), 1.54 (s, 9H), 1.74 (d, $^3J_{\mathrm{PH}} = 17.9$ Hz, 18H), 1.81 (d, $^3J_{\mathrm{PH}} = 17.8$ Hz, 18H), 2.43 (d, $^2J_{\mathrm{PH}} = 9.4$ Hz, 2H), 4.07 (t, J not resolved, 2H); $^{13}\mathrm{C}\{^1\mathrm{H}\}$ NMR (CDCl$_3$): 16.61 (s, CH$_2$), 29.20 (s, $\mathrm{C}(C\mathrm{H_3})_3$), 29.38 (s, $\mathrm{C}(C\mathrm{H_3})_3$), 30.26 (s, $\mathrm{PC}(C\mathrm{H_3})_3$), 30.9 (d, $^2J_{\mathrm{PC}} = 1.5$ Hz, $\mathrm{PC}(C\mathrm{H_3})_3$), 37.56 (dd, $^1J_{\mathrm{PC}} = 11.2$ Hz, $^3J_{\mathrm{PC}} = 3.9$ Hz, $\mathrm{P}C(\mathrm{CH_3})_3$), 37.78 (dd, $^1J_{\mathrm{PC}} = 11.0$ Hz, $^3J_{\mathrm{PC}} = 3.0$ Hz, $\mathrm{P}C(\mathrm{CH_3})_3$), 41.23 (d, $^3J_{\mathrm{PC}} = 4.0$ Hz, $C(\mathrm{CH_3})_3$), 41.48 (d, $^3J_{\mathrm{PC}} = 3.9$ Hz, $C(\mathrm{CH_3})_3$), 41.8 (d, $^1J_{\mathrm{PC}} = 16.0$ Hz, CH$_2$), 177.8 (s, C=N), 189.68 (s, C=N).

*2.2.1.6. $[\mathrm{NiI\{PBu^t_2CH_2C(Bu^t)NNC(Bu^t)CH_2PBu^t_2\}}]\mathrm{I}$ (**2c**).* $^{31}\mathrm{P}\{^1\mathrm{H}\}$ NMR (CDCl$_3$): 79.1, 87.5 (AB system $^2J_{\mathrm{PP}} = 311$ Hz); ^{1}H NMR (CDCl$_3$): 1.37 (s, 18H), 1.65 (d, $^3J_{\mathrm{PH}} = 13.2$ Hz, 18H), 1.70 (d, $^3J_{\mathrm{PH}} = 13.2$ Hz, 18H), 2.31 (d, $^2J_{\mathrm{PH}} = 10.0$ Hz, 2H), 4.08 (t, J not resolved, 2H); $^{13}\mathrm{C}\{^1\mathrm{H}\}$ NMR (CDCl$_3$): 15.51 (s, CH$_2$), 28.22 (s, $\mathrm{C}(C\mathrm{H_3})_3$), 29.22 (s, $\mathrm{C}(C\mathrm{H_3})_3$), 30.23 (s, $\mathrm{PC}(C\mathrm{H_3})_3$), 30.88 (s, $\mathrm{PC}(C\mathrm{H_3})_3$), 37.63 (d, $^1J_{\mathrm{PC}} = 16.9$ Hz, CH$_2$), 38.0 (dd, $^1J_{\mathrm{PC}} = 10.0$ Hz, $^3J_{\mathrm{PC}} = 2.5$ Hz, $\mathrm{P}C(\mathrm{CH_3})_3$), 38.59 (dd, $^1J_{\mathrm{PC}} = 11.7$ Hz, $^3J_{\mathrm{PC}} = 3.4$ Hz, $\mathrm{P}C(\mathrm{CH_3})_3$), 41.23 (d, $^3J_{\mathrm{PC}} = 4.1$ Hz, $C(\mathrm{CH_3})_3$), 41.36 (d, $^3J_{\mathrm{PC}} = 2.3$ Hz, $C(\mathrm{CH_3})_3$), 177.99 (s, C=N), 187.59 (dd, $^2J_{\mathrm{PC}} = 5.9$ Hz, $^4J_{\mathrm{PC}} = 2.3$ Hz, C=N).

*2.2.1.7. $[\mathrm{NiCl\{PPr^i_2CH_2C(Bu^t)NNC(Bu^t)CH_2PPr^i_2\}}]\mathrm{Cl}$ (**3a**).* $^{31}\mathrm{P}\{^1\mathrm{H}\}$ NMR (CDCl$_3$): 62.0; ^{1}H NMR (CDCl$_3$): 1.28 (s, 9H), 1.35 (s, 9H), 1.41–1.60 (m, 24H), 2.41 (b, 2H), 2.46 (m, 4H), 3.9 (b, 2H); $^{13}\mathrm{C}\{^1\mathrm{H}\}$ NMR (CDCl$_3$): 14.53 (bs, CH$_2$), 17.87 (s, CH$_3$), 18.17 (s, CH$_3$), 18.64 (s, CH$_3$), 18.69 (s, CH$_3$), 23.15 (t, $|^1J_{\mathrm{PC}} + {}^3J_{\mathrm{PC}}| = 12$ Hz, CH), 23.76 (t, $|^1J_{\mathrm{PC}} + {}^3J_{\mathrm{PC}}| = 12$ Hz, CH), 27.19 (s, $\mathrm{C}(C\mathrm{H_3})_3$), 28.15 (s, $\mathrm{C}(C\mathrm{H_3})_3$), 33.14 (m, J not resolved, CH$_2$), 40.74 (s, $C(\mathrm{CH_3})_3$), 41.74 (s, $C(\mathrm{CH_3})_3$), 174.81 (s, C=N), 193.49 (s, C=N).

*2.2.1.8. $[\mathrm{NiBr\{PPr^i_2CH_2C(Bu^t)NNC(Bu^t)CH_2PPr^i_2\}}]\mathrm{Br}$ (**3b**).* $^{31}\mathrm{P}\{^1\mathrm{H}\}$ NMR (CDCl$_3$): 64.2, 65.0 (AB system, $^2J_{\mathrm{PP}} = 325$ Hz); ^{1}H NMR (CDCl$_3$): 1.32 (s, 9H), 1.51 (s, 9H), 1.59–1.73 (m, 24H), 2.46 (b, 2H), 2.54 (m, 4H), 3.84 (b, 2H); $^{13}\mathrm{C}\{^1\mathrm{H}\}$ NMR (CDCl$_3$): 16.88 (bs, CH$_2$), 18.40 (s, CH$_3$), 18.91 (s, CH$_3$), 19.13 (s, CH$_3$), 19.45 (s, CH$_3$), 24.11 (m, J not resolved, 2 × CH), 27.31 (s, $\mathrm{C}(C\mathrm{H_3})_3$), 28.78 (s, $\mathrm{C}(C\mathrm{H_3})_3$), 37.10 (m, J not resolved, CH$_2$), 40.54 (s, $C(\mathrm{CH_3})_3$), 41.64 (s, $C(\mathrm{CH_3})_3$), 174.52 (s, C=N), 193.13 (s, C=N).

*2.2.1.9. $[\mathrm{NiI\{PPr^i_2CH_2C(Bu^t)NNC(Bu^t)CH_2PPr^i_2\}}]\mathrm{I}$ (**3c**).* $^{31}\mathrm{P}\{^1\mathrm{H}\}$ NMR (CDCl$_3$): 70.9, 73.0 (AB system, $^2J_{\mathrm{PP}} = 311$ Hz); ^{1}H NMR (CDCl$_3$): 1.29 (s, 9H), 1.39 (dd, $^3J_{\mathrm{HH}} = 7.1$ Hz, $^3J_{\mathrm{PH}} = 14.6$ Hz, 6H), 1.42 (s, 9H), 1.42 (dd, $^3J_{\mathrm{HH}} = 7.3$ Hz, $^3J_{\mathrm{PH}} = 20.6$ Hz, 6H), 1.57 (dd, $^3J_{\mathrm{HH}} = 7.2$ Hz, $^3J_{\mathrm{PH}} = 15.7$ Hz, 6H), 1.60 (dd, $^3J_{\mathrm{HH}} = 6.9$ Hz, $^3J_{\mathrm{PH}} = 15.6$ Hz, 6H), 2.49 ($^2J_{\mathrm{PH}} = 10.1$ Hz, 2H), 2.52 (m, 4H), 3.91(dd, $^2J_{\mathrm{PH}} = 7.3$ Hz, $^2J_{\mathrm{HH}} = 3.5$ Hz, 2H); $^{13}\mathrm{C}\{^1\mathrm{H}\}$ NMR (CDCl$_3$): 15.72 (bs, CH$_2$), 18.57 (s,

Table 2
Crystallographic data for complexes of general formula $[NiX(PR_2CH_2C(Bu^t)NNC(Bu^t)CH_2PR_2)]Y$ (**2a** R = Bu^t, X = Y = Cl; **2b** R = Bu^t, X = Br: **2c** R = Bu^t, X = I; **4a** R = Cy, X = Cl, $X^- = 1/2[NiCl_4]^{2-}$)

	2c	**4a**	**2b**	**2a**
Formula	$C_{28}H_{58}I_2N_2NiP_2 \cdot C_3H_6O$	$C_{36}H_{66}Cl_3N_2Ni_{1.50}P_2$	$C_{28}H_{58}Br_2N_2NiP_2 \cdot CHCl_3$	$C_{28}H_{58}Cl_2N_2NiP_2 \cdot 2CHCl_3$
M	855.42	783.39	822.71	853.15
Crystal system	monoclinic	monoclinic	monoclinic	monoclinic
Space group	$C2/c$	$C2/c$	$C2/c$	$P2_1/n$
a (Å)	27.212(2)	19.862(5)	28.196(5)	11.054(4)
b (Å)	11.981(1)	14.291(3)	11.8507(7)	25.61(2)
c (Å)	24.712(2)	30.20(1)	23.943(2)	15.43(1)
β (°)	102.09(1)	100.19(3)	103.67(1)	99.78(4)
U (Å^3)	7878	8437	7774	4305
Z	8	8	8	4
D_{calc} (g cm^{-3})	1.442	1.233	1.404	1.313
μ (mm^{-1}) (Mo Kα)	2.024	0.967	2.773	0.975
$F(000)$	3488	3352	3400	1784
Number of reflections measured	7075	7627	6948	7853
Number of unique reflections (R_{int})	6874 (0.055)	7399 (0.03)	6801 (0.08)	7562 (0.06)
R_1 ($I > 2\sigma(I)$)	0.04	0.08	0.09	0.07
wR_2	0.11	0.17	0.13	0.11

CH_3), 19.38 (s, CH_3), 19.38 (s, CH_3), 19.80 (s, CH_3), 25.41 (dd, $^1J_{PC} = 22.0$ Hz, $^3J_{PC} = 4.6$ Hz, CH), 25.65 (dd, $^1J_{PC} = 21.1$ Hz, $^3J_{PC} = 3.7$ Hz, CH), 27.46 (s, $C(CH_3)_3$), 28.80 (s, $C(CH_3)_3$), 36.22 (d, $^1J_{PC} = 16.5$ Hz, CH_2), 40.81 (s, $C(CH_3)_3$), 41.76 (d, $^3J_{PC} = 3.7$ Hz, $C(CH_3)_3$), 174.52 (s, C=N), 192.20 (s, C=N).

*2.2.1.10. $[NiCl\{P(C_6H_{11})_2CH_2C(Bu^t)NNC(Bu^t)CH_2P(C_6H_{11})_2\}]_2[NiCl_4]$ (**4a**).* $^{31}P\{^1H\}$ NMR ($CDCl_3$): 53.7; ^1H NMR ($CDCl_3$): 1.20–1.45 (m, 20H), 1.37 (s, 9H), 1.7–2.0 (m, 20H), 2.15–2.30 (m, 4H), 2.39 (b, 2H), 3.89 (b, 2H); $^{13}C\{^1H\}$ NMR ($CDCl_3$): 15.61 (bs, CH_2), 25.59 (s, CH_2), 25.63 (s, CH_2), 26.58 (s, CH_2), 26.91 (s, CH_2), 27.49 (s $C(CH_3)_3$), 27.98 (s, CH_2), 28.03 (s, CH_2), 28.13 (s, CH_2), 28.42 (s, $C(CH_3)_3$), 29.08 (s, CH_2), 32.54 (t, $|^1J_{PC}+^3J_{PC}| = 10$ Hz, CH), 33.67 (t, $|^1J_{PC}+^3J_{PC}| = 10$ Hz, CH), 33.95 (bt, $|^1J_{PC}+^3J_{PC}| = 10$ Hz, CH_2), 40.93 (s, $C(CH_3)_3$), 41.77 (s, $C(CH_3)_3$), 175.37 (s, C=N), 193.19 (s, C=N).

*2.2.1.11. $[NiBr\{P(C_6H_{11})_2CH_2C(Bu^t)NNC(Bu^t)CH_2P(C_6H_{11})_2\}]Br$ (**4b**).* $^{31}P\{^1H\}$ NMR ($CDCl_3$): 64.2; ^1H NMR ($CDCl_3$): 1.25–1.40 (m, 20H), 1.28 (s, 9H), 1.40 (s, 9H) 1.75–2.00 (m, 20H), 2.20–2.35 (m, 4H), 2.42 (b, 2H), 3.91 (b, 2H); $^{13}C\{^1H\}$ NMR ($CDCl_3$): 16.39 (bs, CH_2), 25.62 (s, CH_2), 26.60 (s, CH_2), 26.74 (s, CH_2), 26.86 (s, CH_2), 27.63 (s $C(CH_3)_3$), 28.76 (s, CH_2), 28.76 (s, $C(CH_3)_3$), 28.84 (s, CH_2), 29.44 (s, CH_2), 34.55 (t, $|^1J_{PC}+^3J_{PC}| = 12.7$ Hz, CH), 35.18 (t, $|^1J_{PC}+^3J_{PC}| = 11.7$ Hz, CH), 36.78 (t, $|^1J_{PC}+^3J_{PC}| = 8.7$ Hz, CH_2), 40.87 (s, $C(CH_3)_3$), 41.62 (s, $C(CH_3)_3$), 174.93 (s, C=N), 191.75 (s, C=N).

*2.2.1.12. $[NiI\{P(C_6H_{11})_2CH_2C(Bu^t)NNC(Bu^t)CH_2P(C_6H_{11})_2\}]I$ (**4c**).* $^{31}P\{^1H\}$ NMR ($CDCl_3$): 64.2; ^1H NMR ($CDCl_3$): 1.25–1.40 (m, 20H), 1.29 (s, 9H), 1.38 (s, 9H), 1.75–2.00 (m, 20H), 2.28 (b, 4H), 2.36 (b, 2H), 3.85 (b, 2H); $^{13}C\{^1H\}$ NMR ($CDCl_3$): 16.15 (bt, J not resolved, CH_2), 25.47 (s, CH_2), 26.42 (s, CH_2), 26.53 (s, CH_2), 26.66 (s, CH_2), 27.53 (s, $C(CH_3)_3$), 28.46 (s, $C(CH_3)_3$), 28.59 (s, CH_2), 29.24 (s, CH_2), 34.23 (t, $|^1J_{PC}+^3J_{PC}| = 12.6$ Hz, CH), 34.98 (t, $|^1J_{PC}+^3J_{PC}| = 11.7$ Hz, CH), 36.43 (t, $|^1J_{PC}+^3J_{PC}| = 9.0$ Hz, CH_2), 40.80 (s, $C(CH_3)_3$), 41.46 (s, $C(CH_3)_3$), 175.1 (s, C=N), 191.38 (d, $^2J_{PC} = 5.0$ Hz, C=N).

2.3. X-ray crystallographic analysis

Dark red (**2a**, **2b**) or black (**2c**, **4a**) crystals were mounted in thin-walled glass capillaries and X-ray data collected at r.t. on an Enraf-Nonius MACH3 diffractometer with graphite-monochromatized Mo Kα radiation, using an ω–2θ scan mode. Unit cell dimensions were obtained by least-squares refinement of the setting angles of 25 reflections.

The data were corrected [17] for Lorentz and polarization effects (Lp), for linear decay and empirically for absorption. The heavy atom positions were located by Patterson methods using SHELXS-86 [18]. The remaining atoms were located in successive Fourier-difference maps and refined by least-squares on F^2 using SHELXL-93 [19]. The crystal data are summarized in Table 2.

Solvent molecules were located in the Fourier-difference maps for complexes **2**; chloroform in the cases of **2a** or **2b** or acetone in the case of **2c**.

All the non-hydrogen atoms were refined with anisotropic thermal motion parameters. The hydrogen atoms were included in calculated positions, constrained to ride at fixed distances of the parent carbon atom.

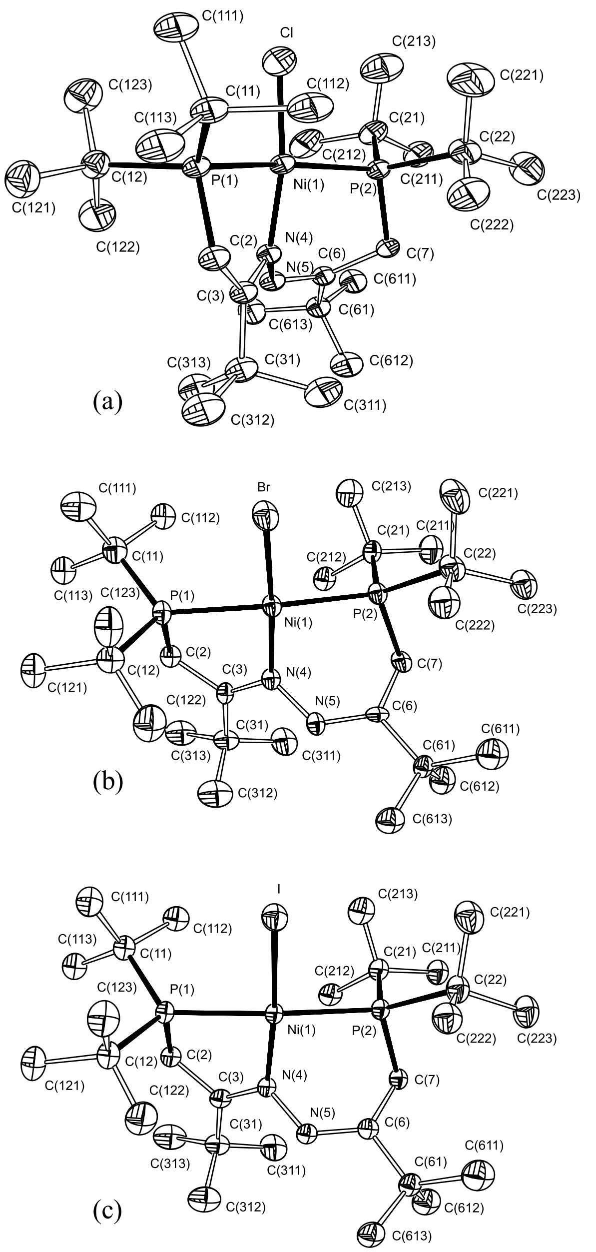

Fig. 1. ORTEP view of molecular structure of (a) $[\mathrm{NiCl}\{\mathrm{PBu^t_2CH_2C(Bu^t)NNC(Bu^t)CH_2PBu^t_2}\}]^+$ in **2a**·2CHCl$_3$, (b) $[\mathrm{NiBr}\{\mathrm{PBu^t_2CH_2C(Bu^t)NNC(Bu^t)CH_2PBu^t_2}\}]^+$ in **2b**·CHCl$_3$, (c) $[\mathrm{NiI}\{\mathrm{PBu^t_2CH_2C(Bu^t)NNC(Bu^t)CH_2PBu^t_2}\}]^+$ in **2c**·(CH$_3$)$_2$CO. Hydrogen atoms are omitted for clarity.

Atomic scattering factors and anomalous dispersion terms were as in SHELXL-93 [19]. The ORTEP drawings were made with ORTEX [20].

3. Results and discussion

3.1. Synthesis and characterization of complexes

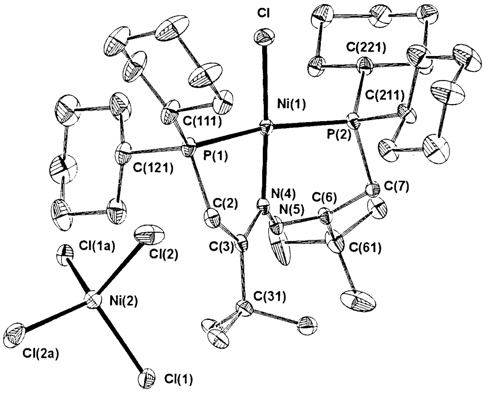

Fig. 2. ORTEP view of molecular structure of $[\mathrm{NiCl}\{\mathrm{P(C_6H_{11})_2CH_2C(Bu^t)NNC(Bu^t)CH_2P(C_6H_{11})_2}\}][\mathrm{NiCl_4}]$ in **4a**. Selected atoms are labeled and hydrogen atoms are omitted for clarity.

The nickel complexes $[\mathrm{NiX}\{\mathrm{PR_2CH_2C(Bu^t)NNC(Bu^t)CH_2PR_2}\}]\mathrm{Y}$ ($\mathrm{R = Ph}$, $\mathrm{X = Cl}$, $\mathrm{Y = 1/2NiCl_4}$ (**1a**); $\mathrm{R = Ph}$, $\mathrm{X = Y = Br}$, I (**1b** or **1c**); $\mathrm{R = Bu^t}$, $\mathrm{X = Y = Cl}$, Br, I (**2a**, **2b**, **2c**); $\mathrm{R = Pr^i}$, $\mathrm{X = Y = Cl}$, Br, I (**3a**, **3b**, **3c**); $\mathrm{R = C_6H_{11}}$, $\mathrm{X = Cl}$, $\mathrm{Y = 1/2[NiCl_4]^{2-}}$ (**4a**); $\mathrm{X = Y = Br}$, I (**4b**, **4c**), were prepared from the corresponding anhydrous nickel(II) halides and azine diphosphines. The best yields were obtained for the nickel bromide derivatives and they tended to increase with the bulkiness of the R group on phosphorus, i.e. $\mathrm{Ph \cong Pr^i} < c\text{-}\mathrm{C_6H_{11}} < \mathrm{Bu^t}$.

The complexes were characterized by conventional techniques (see Section 2). The counterion of the compounds is the halide in all complexes, but for **4a** (verified by X-rays, see Fig. 2) and **1a** (on the basis of elementary analysis and negative FAB) it is $[\mathrm{NiCl_4}]^{2-}$.

Apart from complexes $[\mathrm{NiX}\{\mathrm{PPh_2CH_2C(Bu^t)NNC(Bu^t)CH_2PPh_2}\}]^+$ (**1**) all the species display well defined NMR spectra consistent with their formulation. In the case of complexes **1a** and **1b** the ^{1}H and ^{31}P NMR spectra are so broad that no attribution of the signals could be made.

The ^{1}H and ^{31}P NMR spectra of complexes **2**, **3** and **4** suggest that no appreciable structural differences exist between them. In addition, the spectra of **1c** and that of Pd(II) complex [11] with the analogous bis(diphenylphosphino)pinacolone azine ligand are quite similar in what concerns the coordination of the phosphine, i.e. the *trans* coordination of the two phosphorus atoms is confirmed by a large $^2J_{\mathrm{PP}}$ coupling constant (ca. 330 Hz). The asymmetry of the two moieties of the azine diphosphine ligand caused by the formation of two non-equivalent five- and a six-membered rings is clearly identified in the proton and carbon NMR spectra by distinct signals of all relevant (Bu^t, CH$_2$, C=N) groups in the two rings.

The broadness of the NMR spectra of **1a** and **1b** is consistent with paramagnetic character and suggests these complexes have an electronic and geometric structure considerably different from the other compounds under study. A distortion from the essentially

Table 3
Selected bond lengths (Å) and angles (°) with e.s.d.s in parentheses for **2a**–**c** and **4a**

	4a	**2a**	**2b**	**2c**
Bond lengths				
Ni–P(1)	2.192(3)	2.196(2)	2.202(4)	2.213(2)
Ni–P(2)	2.199(2)	2.246(2)	2.260(4)	2.268(2)
Ni–N(4)	1.903(6)	1.916(4)	1.897(10)	1.926(5)
Ni–X	2.157(3)	2.148(3)	2.300(2)	2.4882(9)
Bond angles				
P(1)–Ni–N(4)	83.0(2)	84.7(2)	84.3(3)	84.2(2)
P(1)–Ni–X	95.7(1)	91.74(8)	92.5(1)	92.29(5)
P(2)–Ni–N(4)	91.2(2)	92.6(2)	90.7(3)	90.6(2)
P(2)–Ni–X	90.9(1)	93.28(7)	95.9(1)	96.77(5)
P(1)–Ni–P(2)	165.4(1)	163.9(1)	160.1(2)	159.8(1)
N(4)–Ni–X	176.2(2)	170.4(1)	168.4(3)	167.1(1)

square-planar structure (diamagnetic), confirmed by X-rays on complexes **2a**, **2b**, **2c**, Fig. 1, and **4a**, Fig. 2, towards a tetrahedral (paramagnetic) geometry, in the case of the phenyl substituent (R) on the phosphine arm would explain the paramagnetic behavior of **1a** and **1b**. The absence of an appreciable paramagnetic effect, in the case of complex **1c**, for which reasonable NMR spectra could be obtained, points to the magnitude of the square-planar to tetrahedral distortion being controlled by the bulkiness of the X group.

We were unable to detect EPR signals in complexes **1**, either at r.t. or at low (−196 °C) temperatures. However, the effective magnetic moment values measured at r.t. on complexes **1a** (2.57 μ_B) and **1b** (2.2 μ_B), although lower than the expected spin only value for two unpaired electrons (2.83 μ_B) [21], are still acceptable as an evidence of paramagnetic character. The measurement of the magnetic susceptibility of **1c** gave inconsistent results. The μ_{eff} values measured for the phenyl substituted diphosphine azine nickel complexes **1** point to an increasing tendency to distort from square planar to tetrahedral geometry in the order I < Br < Cl.

This is exactly the inverse trend to that observed in the azine diphosphine nickel complexes with non-aromatic R groups, Table 2, structurally characterized within this study that display square-planar geometries, with a degree of tetrahedral distortion that increases with the bulkiness of the coordinated halide, Table 3.

Unfortunately, no X-ray diffraction data could be obtained for complexes **1**, due to crystal disorder, although apparently good crystals of **1a** were obtained.

From the above mentioned data obtained by NMR, magnetic susceptibility and X-rays it seems there is a fine balance between square-planar and tetrahedral geometry in $[NiX\{PR_2CH_2C(Bu^t)NNC(Bu^t)CH_2PR_2\}]^+$ ions. The square-planar versus tetrahedral geometry is unexpected for the bulkier iodide compared with chloride in complexes **1**, such as it is in the case of the bulkier R groups in complexes **2**–**4**, compared with phenyl. The results herein suggest a significant dependence of the geometry on electronic effects.

The geometry/magnetic properties herein are in full agreement with those of other nickel(II) phosphine complexes [22] that, in the case of R = alkyl and the bulky iodide ligand, display a tendency to diamagnetic planar forms, whereas in the case of R = aryl and the less steric demanding chloride ligand a paramagnetic tetrahedral form is preferred.

In the azine diphosphine nickel complexes **1** there is a considerably lower electron density at the metal site (see electrochemical studies) than at the complexes **2**–**4**. These electronic properties conceivably are related to the geometry of the species (tetrahedral for X = Cl or Br). In the case of **1c**, the electronic properties do not contribute much to the square-planar geometry, since iodide behaves essentially as a non π-electron donor.

3.2. Structural studies

The molecular structures of the bis(di-*t*-butylphosphino)pinacolone azine complexes, **2a**–**c**, Fig. 1, as well as that of the cyclohexyl analogue **4a**, Fig. 2, were obtained by single crystal X-ray diffraction.

All the complexes show a square planar geometry with some degree of distortion.

Selected bond lengths and angles are listed in Table 3.

From the available structural data it is evident that the Ni–P1 bond lengths in the six-membered rings are longer than the corresponding Ni–P2 bond lengths in the five-membered rings, although in the case of complex **4a** the effect is very small. This small effect is responsible for the small difference in the value of the ^{31}P NMR chemical shifts observed for the two phosphorus atoms in complexes **4** that becomes comparable to the coupling constant and consequently the usual ^{31}P AB system (of the other Ni diphosphine azine complexes) collapses into a single line.

In order to rationalize the structural parameters summarized in Table 3 some extended low level Hückel MO calculations were performed using as crude model the undistorted square-planar $[trans\text{-}NiX(NH_2)(PH_3)_2]^+$. We would like to emphasize that these calculations are used just to qualitatively analyze the structural trends and do not aim at any quantitative estimate of structural parameters or energies.

The results of the calculations are depicted in Fig. 3. The analysis of these results shows that the contribution of the halide to the π-system drops in the series Cl > Br > I and almost vanishes in the case of iodide. This is also the trend observed for the differences of the Ni–P bond lengths in the two metallacycles. Moreover, the geometry of the two metallacycles imposes a 5° decrease in the P1–Ni–N angle (~ 85°) that improves the overlap population of π-orbitals of the halide with the *xz* metal

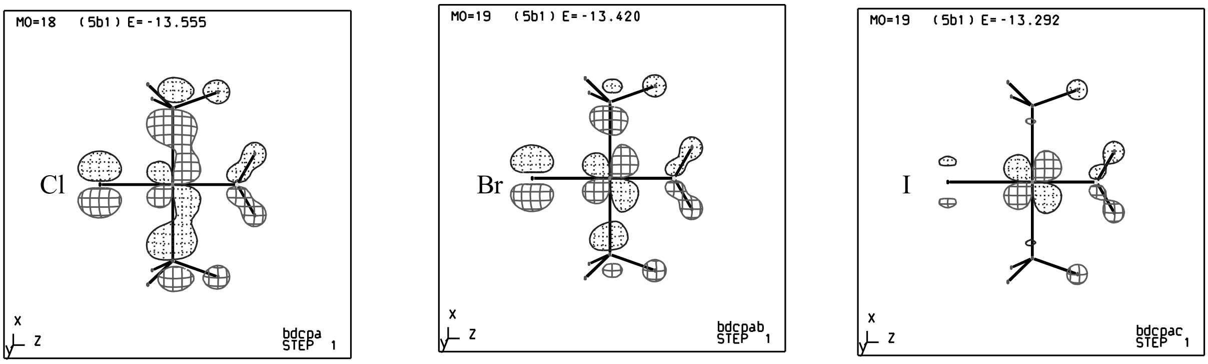

Fig. 3. CACAO MO drawings depicting the halogen π-bonding for an ideal square planar Ni–X (X = Cl, Br or I) geometry.

orbital, further decreasing the Ni–P1 distance when compared with a corresponding Ni–P2 bond length.

From these qualitative results, it comes out that the π interactions may be responsible for the observed trends, since the analysis of the in plane π interactions and the contribution of the Ni–P σ electron density for the model complex, Fig. 3, shows that there is a tendency to shorter Ni–P1 compared with Ni–P2 bond lengths as well as a dependence of the Ni–P bond length on the characteristics of the coordinated halide.

In order to compare the distortion from the square-planar geometry, induced by the R groups in the phosphine ligand, the angle defined by the plane formed by the metal and the two ligand sites in the five-membered ring and the plane that contains the metal, the halogen and the phosphorus atoms, in the six-membered ring, was calculated. The obtained values for **4a** (13.8°), **2a** (17.9°), **2b** (21.5°) and **2c** (22.3°) show that the distortions from the square-planar geometry increase with the bulkiness of the R and the X groups. The higher distortion imposed by the bulkier *tert*-butyl compared with the cyclohexyl group is consistent with their relative bite angles (P–Ni–P), Table 3.

A tentative rationalization of the degree of distortion imposed by the halide, in complexes **2**, was also made on the basis of the calculation of the difference between the sum of the P1–Ni–N plus P2–Ni–N angles and the P1–Ni–P bite angle. The values vary from 13.4° (Cl) to 14.9° (Br) and 15.0° (I), in agreement with a bigger distortion in the case of the bulkier halide. The $^2J_{PP}$ values measured by NMR in **2a** (325 Hz), **2b** (322 Hz) and **2c** (311 Hz) provide a spectroscopic evidence for this distortion.

3.3. Electrochemical studies

The electrochemical behaviors of the complexes **1**–**4**, and that of the free azine diphosphine ligands were studied by cyclic voltammetry in 0.2 M $[NBu_4][BF_4]$–THF or dichloromethane solutions using a Pt wire as the working electrode, and the obtained experimental data are displayed in Table 4.

As a general trend, the complexes display one reversible reduction wave (I) followed by an irreversible one (II) at a lower potential. In addition, two anodic processes are observed for the complexes with bromide or iodide as the counterion, which were attributed to the halide oxidation, Table 4. Controlled potential electrolysis performed at the reduction potential of wave (I) on complexes **1b** and **1c** is consistent with one electron per molecule in the processes.

The free azine diphosphines, $PR_2CH_2C(Bu^t)NNC(Bu^t)CH_2PR_2$, display by cyclic voltammetry one anodic irreversible process at potentials considerably dependent on the R group, Table 4.

3.3.1. Cathodic behavior

The reversible cathodic wave (I) observed with complexes **1**, **2** and **3** (in THF) and **4** (in CH_2Cl_2) is attributed to the Ni(II) → Ni(I) reduction process in agreement with the results obtained by controlled potential electrolysis.

In THF the electrochemical behavior of the cyclohexyl diphosphine azine complexes **4** differs considerably from that of the other complexes, due to slow decomposition and the instability of the reduced species that leads to the irreversibility of wave (I). However, in CH_2Cl_2, a solvent with lower coordination ability, the characteristics of wave (I) follow that of the other complexes in THF.

The complexes **1** with the aromatic R group are reduced at a less cathodic potential than those with the alkyl R group (**2**–**4**), in agreement with the expected weaker electron-donor character of the aromatic azine diphosphine ligand. However, the difference may be accounted for by a different geometry. It is also observed that the aryl or alkyl nature of the R group on the diphosphine azine ligands plays an important role on the potentials of the cathodic processes. In addition, the halogen ligands have a marked influence on the redox potentials of the R = alkyl complexes **2**–**4**, but not in the R = aryl complexes **1**.

The reduction potential values of wave (I) in complexes **2**–**4**, follow the order Cl < Br < I, which is the inverse

Table 4
Cyclic voltammetry data [a] for complexes $[NiX(PR_2CH_2C(Bu^t)NNC(Bu^t)CH_2PR_2)]^+$ and diphosphine azines $PR_2CH_2C(Bu^t)NNC(Bu^t)CH_2PR_2$

R	X		Cathodic		Anodic		
			Complex		Complex		Free diphosphine
			${}^{I}E_{1/2}^{red}$	${}^{II}E_{p}^{red}$	${}^{I}E_{p}^{ox}$	${}^{II}E_{1/2}^{ox}$	E_{p}^{ox}
Ph	Cl	**1a**	−0.45	−1.63		[b]	1.22
	Br	**1b**	−0.44	−1.67	0.74	1.06	
	I	**1c**	−0.43	−1.62	0.33	0.63	
Bu^t	Cl	**2a**	−0.71	−1.66			1.18
	Br	**2b**	−0.61		0.79	1.01 [c]	
	I	**2c**	−0.52	−1.44	0.34	0.64	
Pr^i	Cl	**3a**	−0.75	−1.32			1.46
	Br	**3b**	−0.68 [c]	−1.60	0.74	1.09 [d]	
	I	**3c**	−0.62	−1.96	0.31	0.62	
C_6H_{11}	Cl	**4a**	−0.71 [d]	−1.26		[b]	1.42
	Br	**4b**	−0.66 [d]	−1.53	0.87	1.09	
	I	**4c**	−0.63 [d]	−1.65	0.35	0.65	

[a] Potential values in volts (±20 mV) vs. SCE, measured in 0.2 M $[NBu_4][BF_4]$–THF, unless stated otherwise, at 200 mV s^{-1}, using $[Fe(\eta^5\text{-}C_5H_5)_2]^{0/+}$ ($E_{1/2}^{ox} = 0.54$ V, vs. SCE).
[b] The counterion is $[NiCl_4]^{2-}$.
[c] $E_{p/2}^{red}$.
[d] Values measured in CH_2Cl_2.

order of the net π-electron donor ability of the halide ligand (see Fig. 3). Moreover, within the compounds with alkyl R groups the potentials of the Ni(II) → Ni(I) process, for the same halide ligand, are little dependent on the R group. In fact, the potentials of complexes **2a** (−0.71 V), **3a** (−0.75 V), **4a** (−0.71 V), for which the coordinated halogen is chloride, do not differ much. The same trend is verified for bromide and, as expected (see above), in a lesser extent for iodide, Table 4. Hence, for complexes **2**–**4** (with the alkyl R group) the electronic characteristics of the halide present a dominant effect on their redox properties. However, this behavior is no longer found in complexes **1** for which the potentials of wave (I) are independent of the coordinated halide and higher than those of complexes **2**–**4**.

The results herein indicate that for the square-planar geometry (which, as shown by the above theoretical studies, enables the participation of the halide in the LUMO of the complexes) the redox properties of the $[NiX\{PR_2CH_2C(Bu^t)NNC(Bu^t)CH_2PR_2\}]^+$ complexes become highly dependent on X and almost independent of R. A balance between steric and electronic effects operate in these Ni–diphosphine azine complexes which corroborates that mentioned for other Ni(II) systems [22].The cathodic waves (II) display potential values that tend to follow the same trend as wave (I), although the process is irreversible.

In order to fully confirm conclusions suggested herein, the study needs to be extended to other R groups.

3.3.2. *Anodic behavior*

Two anodic processes are detected in all the complexes except those with chloride or $[NiCl_4]^{2-}$ as counterions. Typically a lower potential irreversible process followed by a higher potential reversible process was detected, Table 4, which were attributed to the oxidation of the halide counterion.

The free azine diphosphines $PR_2CH_2C(Bu^t)NNC(Bu^t)CH_2R_2$ display in THF–$[NBu_4][BF_4]$, ill-defined anodic processes. In CH_2Cl_2 at least one reasonably well-defined anodic wave is observed at potential values highly dependent on the R group, Table 4. The oxidation potentials of the diphosphine azines do not follow directly the electronic or steric properties of the R substituents. Moreover, there is no evident relationship between the oxidation potentials of the free phosphines and the potential of the Ni(II) → Ni(I) reduction process.

Acknowledgements

The authors thank Mr. Jan Storch for skillful experimental assistance. This project was supported by the Grant Agency of the Czech Republic (grant No. 203/01/0554), the Fundação para a Ciência e Tecnologia (FCT, POCTI/36125/QUI/99) and the ICCTI/ASCR Protocol (ICCTI/ACCR-432/AC.C.Rep.Checa, by a travel grant).

References

[1] R.A. Gossage, L.A. Vandekuil, G. van Koten, Acc. Chem. Res. 31 (1998) 423.

[2] J.G. Donkervoort, J.L. Vicario, J.T.B.H. Jastrzebski, R.A. Gossage, G. Cahiez, G. van Koten, J. Organomet. Chem. 558 (1998) 61.

[3] B. Rybtchinski, D. Milstein, Angew. Chem., Int. Ed. 38 (1999) 871.

[4] M.E. van der Boom, Y. Ben David, D. Milstein, J. Am. Chem. Soc. 121 (1999) 6652.

[5] M.E. van der Boom, J. Ott, D. Milstein, Organometallics 17 (1998) 4263.

[6] M. Gandelman, A. Vigalok, L.J.W. Shimon, D. Milstein, Organometallics 16 (1997) 3981.

[7] J. Vicente, A. Arcas, M.A. Blasco, J. Lozano, M.C.R. Dearellano, Organometallics 17 (1998) 5374.

[8] D.E. Bergbreiter, P.L. Osburn, Y.S. Liu, J. Am. Chem. Soc. 121 (1999) 9531.

[9] P.C.J. Kamer, J.N.H. Reek, P.W.N.M. van Leeuwen, Chemtech 28 (1998) 27.

[10] S.D. Perera, B.L. Shaw, M. Thornton-Pett, J. Chem. Soc., Dalton Trans. (1992) 1469.

[11] S.D. Perera, B.L. Shaw, M. Thornton-Pett, J. Chem. Soc., Dalton Trans. (1993) 3653.

[12] S.D. Perera, B.L. Shaw, M. Thornton-Pett, J. Chem. Soc., Dalton Trans. (1994) 3311.

[13] S.D. Perera, B.L. Shaw, M. Thornton-Pett, J. Chem. Soc., Dalton Trans. (1996) 3111.

[14] M.F.N.N. Carvalho, M.T. Duarte, A.M. Galvão, A.J.L. Pombeiro, J. Čermák, S. Šabata, P. Vojtíšek, J. Podlaha, J. Organomet. Chem. 598 (2000) 318.

[15] J. Čermák, M. Kvíčalová, S. Šabata, V. Blechta, P. Vojtíšek, J. Podlaha, B.L. Shaw, Inorg. Chim. Acta 313 (2001) 77.

[16] G.W. Watt, P.S. Gentile, E.P. Helvenston, J. Am. Chem. Soc. 77 (1955) 2752.

[17] C.K. Fair, MOlEN. Enraf-Nonius, Delft, 1990.

[18] G.M. Sheldrick, SHELXS 86, Program for the Solution of Crystal Structure, University of Göttingen, Göttingen, Germany, 1986.

[19] G.M. Sheldrick, SHELXL 93, Program for the Refinement of Crystal Structure, University of Göttingen, Göttingen, Germany, 1993.

[20] P. McArdle, J. Appl. Crystallogr. 28 (1995) 65.

[21] A.G. Sharp, Inorganic Chemistry, Longman, London, 1981, p. 487.

[22] N.N. Greenwood, A. Earnshaw, Chemistry of the Elements, Pergamon Press, Oxford, 1990, pp. 1346–1347.